Electron-impact ionization of the oxygen atom

Sunggi Chung and Chun C. Lin
Department of Physics, University of Wisconsin, Madison, Wisconsin 53706

Edward T. P. Lee
Phillips Laboratory (Air Force Systems Command), Bedford, Massachusetts 01731
(Received 28 September 1992)

The cross sections for electron-impact ionization of oxygen atoms in the $(2p^4)^3P$ ground state to form O^+ ions in the $(2p^3)^4S$, $(2p^3)^2D$, and $(2p^3)^2P$ states have been calculated by the Born-Ochkur approximation for incident-electron energies from the threshold to 500 eV and by the method of exchange distorted waves (with Ochkur's approximation) from the threshold to 200 eV. Comparisons are made with previous theoretical calculations and with experimental measurements. Our calculated cross sections agree well with the experimental values, the difference being about 15% at energies above 50 eV. The contributions from autoionization and from the inner-shell ionization (by removing the 2*s* electron) are also discussed. The cross-section calculation is extended to ionization of oxygen atoms in the $[2p^3(^4S)n_0l_0]^3L_0$ excited states by means of the Born-Ochkur approximation for n_0l_0 up to (6,5) and the method of distorted waves for $n_0l_0=3s$, $3p$, and $3d$.

PACS number(s): 34.80.Dp

I. INTRODUCTION

Electron-impact ionization of the oxygen atom is an important basic process in atmospheric and plasma physics. Experimental measurements of ionization of atoms (including oxygen) and molecules have been reviewed by Kieffer and Dunn [1]. More recent compilations of ionization data are given by Laher and Gilmore [2], and by Bell *et al.* [3]. The electron-impact ionization cross sections of the oxygen atom were measured by Fite and Brackmann [4], Rothe *et al.* [5], Brook, Harrison, and Smith [6], and Zipf [7]. In the first two experiments [4,5] a partially dissociated oxygen beam containing O_2 and O was used to measure the ratio of the ionization cross sections of the two species $\sigma(O^+)/\sigma(O_2^+)$, which, upon combining with the total molecular ionization cross sections of Tate and Smith [8], gives $\sigma(O^+)$. Brook, Harrison, and Smith [6] used the charge-exchange process as the source of atomic oxygen beam. Zipf [7] used a beam of O-O_2 mixture, but the normalization procedure was different. Zipf [7] also revised the data of Fite and Brackmann [4] using the newer O_2 ionization cross sections of Mark [9].

An early calculation of ionization cross sections of oxygen atoms [10] was made by utilizing the relationship between the electron-impact and photoionization cross sections. Subsequent calculations [11–16] involve the Born approximation, and in all but one case [16] the hydrogenic Coulomb functions were used to describe the ionized electrons and the 2*p* atomic wave functions were obtained by various means. The Coulomb functions were orthogonalized to the 2*p* function by the customary (but somewhat arbitrary) procedure. Peach [11] used the 2*p* function of Clementi [17], and computed the cross sections with both the Born and Born-Ochkur approximations. Other kinds of 2*p* atomic wave functions were used in Refs. [13–15] as explained in the respective papers. Burnett and Rountree [16] computed the ionization cross sections by the Born approximation with no allowance for the electron exchange, but with a set of wave functions much more elaborate than the ones used in other works [11–15]. For the initial state of the target atom, a six-term configuration-interaction (CI) wave function is used to describe the ground state of the oxygen atom $O(^3P)$. The continuum wave functions for the ejected electron in the final target state are determined by solving the close-coupling equations that result from the inclusion of the ^4S, ^2D, and ^2P terms of the $2p^3$ configuration of the free O^+ ion in the Schrödinger equation for the target.

In this paper we conduct a systematic theoretical study for the electron-impact ionization of the oxygen atom from the excited states as well as from the ground state. We start with the Born approximation to calculate the ionization cross section of the ground-state $O(^3P)$ oxygen atoms, and treat the electron exchange using the procedure suggested by Ochkur [18], i.e., the Born-Ochkur approximation. To improve the cross sections at low energies, we replace the Born-type approximation by the method of (exchange) distorted waves with Ochkur's exchange. The calculation is extended to some low-lying excited oxygen atoms in the $2p^3(^4S)n_0l_0\,^3L_0$ states. To calculate the wave functions, we use the frozen-core approximation by which we assume that the 1*s*, 2*s*, and 2*p* functions remain unchanged in the $O(^3P)$, $O[(^4S)n_0l_0\,^3L_0]$, and $O^+(^4S,^2D,^2P)$ states. The wave functions of the excited orbitals n_0l_0, of the ejected electron, and of the distorted projectile electron are computed by the Hartree-Fock procedure while those of 1*s*, 2*s*, and 2*p* are taken from the paper of Clementi and Roetti [19].

In Sec. II we set the theoretical framework under which the cross sections are calculated. In Sec. III we present the results and compare them with previous theoretical calculations and with the experimental measurements. Section IV concludes the paper.

II. THEORY

A. General description and the Born-Ochkur approximation

Since the theory of electron-impact ionization of atoms has been treated extensively by Peterkop [20], Rudge and Seaton [21], and Rudge [22], we will cite the relevant results developed in those papers without detailed explanations. Let us first consider the simplest case of e-H ionizing collision where an incident electron of momentum $\hbar\mathbf{k}_0$ impinges on the hydrogen atom of wave function $\phi_0(\mathbf{r}_2)$ resulting in a scattered electron of momentum $\hbar\mathbf{k}_1$ and an ionized electron of momentum $\hbar\mathbf{k}_2$. The kinetic energies of the electrons are related as

$$k_0^2-2I=k_1^2+k_2^2 , \tag{1}$$

where I is the ionization potential energy in a.u. The bound-state function $\phi_0(\mathbf{r})$ is expressed as

$$\phi_0(\mathbf{r})=R_{n_0l_0}(r)Y_{l_0m_0}(\hat{\mathbf{r}})=r^{-1}P_{n_0l_0}(r)Y_{l_0m_0}(\hat{\mathbf{r}}) , \tag{2}$$

and the wave function of the ionized electron $\phi(\mathbf{k}_2,\mathbf{r})$ as

$$\phi(\mathbf{k}_2,\mathbf{r})=\sum_{l=0}^{\infty}\sum_{m=-l}^{l}R_{\varepsilon l}(r)Y_{lm}(\hat{\mathbf{r}})Y_{lm}(\hat{\mathbf{k}}_2) . \tag{3}$$

Here we used the symbol ε, which is $k_2^2/2$, to indicate the energy of the ionized electron. As indicated in Eq. (2) we use $P_{nl}(r)$ to designate the "reduced" radial wave function $rR_{nl}(r)$. The cross sections of this process are dictated by the direct and exchange amplitudes $f(\mathbf{k}_1,\mathbf{k}_2)$ and $g(\mathbf{k}_1,\mathbf{k}_2)$. Discussions of f and g can be found in, for example, the paper by Rudge and Seaton [21] where the symbols $\mathbf{k}$ and $\mathbf{k}'$ are used in place of our $\mathbf{k}_1$ and $\mathbf{k}_2$. The ionization cross section integrated over all directions of $\mathbf{k}_1$ and $\mathbf{k}_2$ is given by

$$\left[\frac{d\sigma}{d\varepsilon}\right]^{\pm}=(k_1k_2/k_0)\int|f(\mathbf{k}_1,\mathbf{k}_2)\pm g(\mathbf{k}_1,\mathbf{k}_2)|^2d\hat{\mathbf{k}}_1d\hat{\mathbf{k}}_2 , \tag{4}$$

where the superscripts + and − on the left-hand side correspond to scattering states with total spin 0 and 1, respectively. If the H atom is ionized by unpolarized electrons, then the cross section is the weighted average of the + and − with the statistical weight 1:3.

In the Born approximation (with no exchange), the g term is neglected and the f term is approximated by

$$f(\mathbf{k}_1\mathbf{k}_2)\simeq-(1/2\pi)\int e^{i\mathbf{k}_0\cdot\mathbf{r}_1}\phi_0(\mathbf{r}_2)|\mathbf{r}_1-\mathbf{r}_2|^{-1}\times e^{-i\mathbf{k}_1\cdot\mathbf{r}_1}\phi^*(\mathbf{k}_2,\mathbf{r}_2)d\mathbf{r}_1d\mathbf{r}_2 , \tag{5}$$

where $\phi_0(\mathbf{r}_2)$ and $\phi(\mathbf{k}_2,\mathbf{r}_2)$ are defined in Eqs. (2) and (3). Alternatively, one can adopt the Born-Oppenheimer approximation in which g is taken from Eq. (5) by permuting the two electrons in the final state, i.e.,

$$g(\mathbf{k}_1,\mathbf{k}_2)=-(1/2\pi)\int e^{i\mathbf{k}_0\cdot\mathbf{r}_1}\phi_0(\mathbf{r}_2)|\mathbf{r}_1-\mathbf{r}_2|^{-1}\times e^{-i\mathbf{k}_1\cdot\mathbf{r}_2}\phi^*(\mathbf{k}_2,\mathbf{r}_1)d\mathbf{r}_1d\mathbf{r}_2 . \tag{6}$$

The use of the Born-Oppenheimer exchange amplitude of Eq. (6) leads to the well-known difficulty of overestimating the cross sections especially at incident energies near the threshold. Ochkur [18] has suggested an approximation for treating the exchange amplitude for ionization processes, i.e.,

$$g(\mathbf{k}_1,\mathbf{k}_2)\simeq f(\mathbf{k}_1,\mathbf{k}_2)|\mathbf{k}_0-\mathbf{k}_1|^2/(k_0^2-k_2^2) . \tag{7}$$

This Born-Ochkur (BO) approximation is shown to yield much closer agreement with experiment for e-H ionization than the Born approximation or the Born-Oppenheimer approximation [18]. In the present work we shall use Eq. (7) to compute exchange amplitude yielding

$$\left[\frac{d\sigma}{d\varepsilon}\right]^{\pm}_{\mathrm{BO}}=(k_1k_2/k_0)\int(X^{\pm})^2|f(\mathbf{k}_1\mathbf{k}_2)|^2d\hat{\mathbf{k}}_1d\hat{\mathbf{k}}_2 , \tag{8}$$

with

$$X^{\pm}=1\pm|\mathbf{k}_0-\mathbf{k}_1|^2/(k_0^2-k_2^2) . \tag{9}$$

Following Peterkop [20], we evaluate Eq. (8) by reexpressing $f(\mathbf{k}_1,\mathbf{k}_2)$ of Eq. (5) as

$$f(\mathbf{k}_1,\mathbf{k}_2)=-2K^{-2}\langle 0|\mathbf{K}|\mathbf{k}_0\rangle , \tag{10}$$

$$\mathbf{K}=\mathbf{k}_0-\mathbf{k}_1 , \tag{11}$$

$$\langle 0|\mathbf{K}|\mathbf{k}_2\rangle=\int\phi_0(\mathbf{r}_2)e^{i\mathbf{K}\cdot\mathbf{r}_2}\phi^*(\mathbf{k}_2,\mathbf{r}_2)d\mathbf{r}_2 . \tag{12}$$

Integration over $d\hat{\mathbf{k}}_1$ and $d\hat{\mathbf{k}}_2$ reduces Eq. (8) to

$$\left[\frac{d\sigma}{d\varepsilon}\right]^{\pm}_{\mathrm{BO}}=8\pi k_0^{-2}\int_{K_{\min}}^{K_{\max}}(X^{\pm})^2|\langle n_0l_0|K|\varepsilon\rangle|^2K^{-3}dK , \tag{13}$$

$$|\langle n_0l_0|K|\varepsilon\rangle|^2=(2l_0+1)^{-1}\sum_{m_0,l,m}\left|\int R_{n_0l_0}(r)Y_{l_0m_0}(\hat{\mathbf{r}})\times e^{i\mathbf{K}\cdot\mathbf{r}}R_{\varepsilon l}(r)Y_{lm}^*(\hat{\mathbf{r}})d\mathbf{r}\right|^2 . \tag{14}$$

The integration limits $K_{\min}$ and $K_{\max}$ in Eq. (13) are the (absolute value of) difference and sum of k_0 and k_1, respectively. The cross sections are averaged over the initial magnetic substrates m_0 as indicated in Eq. (14). The total ionization cross section is

$$\sigma^{\pm}(E)=\int_0^{E_{\max}/2}\left[\frac{d\sigma}{d\varepsilon}\right]^{\pm}d\varepsilon , \tag{15}$$

where E is the incident-electron energy and

$$E_{\max}=E-|I|-k_1^2/2 \ . \tag{16}$$

The upper limit in Eq. (15) is set to $E_{\max}/2$ instead of $E_{\max}$, since a close examination [20–22] shows that $g(\mathbf{k}_2,\mathbf{k}_1)$ and $f(\mathbf{k}_1,\mathbf{k}_2)$ describe the same physical occurrence. To avoid this redundancy, the upper limit in Eq. (15) is set to $E_{\max}/2$.

Comparison of the BO cross sections for ionization of the H atom with those obtained by the Born approximation shows that inclusion of exchange does not greatly alter the cross sections except at low energies. For example, by reading the figure in Ref. [18], we see that the ratios of the BO cross sections to the Born cross sections are about 0.65, 0.75, 0.83, and 0.89 at 25, 50, 100, and 200 eV, respectively.

B. Method of distorted waves

In the Born approximation, plane waves $e^{i\mathbf{k}_0\cdot\mathbf{r}}$ and $e^{i\mathbf{k}_1\cdot\mathbf{r}}$ are used for the incident and scattered waves. Because of the interaction of the projectile electron with the target atomic electrons and nucleus, departure from plane wave is expected. The method of distorted wave (DW) attempts to correct for this departure, and has been applied to electron-impact excitations and ionization of atoms [23–25]. To simplify the formulation we may, without loss of generality, assume the direction of the incident electron to be the z direction. With allowance for distortion by the target, the incident-electron function is expanded as

$$\phi(\mathbf{k}_0,\mathbf{r})=(4\pi)^{1/2}\sum_{l_1} i^{l_1}(2l_1+1)^{1/2}r^{-1}\mathcal{P}_{k_0 l_1}(r)Y_{l_1 0}(\hat{\mathbf{r}}) \ , \tag{17}$$

while the scattered-wave function is expanded as

$$\phi(\mathbf{k}_1,\mathbf{r})=4\pi\sum_{l_2,m_2} i^{l_2}r^{-1}\mathcal{P}_{k_1 l_2}(r)Y_{l_2 m_2}(\hat{\mathbf{r}})Y^*_{l_2 m_2}(\hat{\mathbf{k}}_1) \ , \tag{18}$$

where $r^{-1}\mathcal{P}_{kl}(r)$ denotes the distorted partial waves which are the solutions of the Schrödinger equation for the incident (or scattered) electron in the field of the hydrogen atom. The precise form of the differential equation for the distorted partial waves will be given in Sec. II C, when we discuss the electron-impact ionization of the oxygen atom [Eq. (42)]. To obtain the DW scattering amplitude we substitute Eqs. (17) and (18) for $e^{i\mathbf{k}_0\cdot\mathbf{r}_1}$ and $e^{i\mathbf{k}_1\cdot\mathbf{r}_1}$, respectively, in Eq. (5), along with

$$\frac{1}{|\mathbf{r}_1-\mathbf{r}_2|}=\frac{1}{r_>}\sum_{\lambda,u}\left[\frac{4\pi}{2\lambda+1}\right]\left[\frac{r_<}{r_>}\right]^{\lambda}Y^*_{\lambda\mu}(\hat{\mathbf{r}}_1)Y_{\lambda\mu}(\hat{\mathbf{r}}_2) \ . \tag{19}$$

The DW direct amplitude becomes

$$f(\mathbf{k}_1,\mathbf{k}_2)=-4\sqrt{\pi}\sum_{l_1,l_2,m_2} i^{l_1-l_2}(2l_1+1)^{1/2}\sum_{\lambda}c^{\lambda}(l_1 0,l_2 m_2)c^{\lambda}(lm,l_0 m_0)Y^*_{lm}(\hat{\mathbf{k}}_2)Y^*_{l_2 m_2}(\hat{\mathbf{k}}_1)R^{\lambda}(k_0 l_1,n_0 l_0,k_1 l_2,nl) \ , \tag{20}$$

where, as defined by Condon and Shortley [26],

$$c^{\lambda}(l_1 m_1,l_2 m_2)=[4\pi/(2\lambda+1)]^{1/2}\int Y^*_{l_1 m_1}(\hat{\mathbf{r}})Y_{\lambda,m_1-m_2}(\hat{\mathbf{r}})Y_{l_2 m_2}(\hat{\mathbf{r}})d\hat{\mathbf{r}} \ , \tag{21}$$

and

$$R^{\lambda}(k_0 l_1,n_0 l_0,k_1 l_2,nl)=\int_0^{\infty}\mathcal{P}_{k_0 l_1}(r)\mathcal{P}_{k_1 l_2}(r)dr\left[r^{-\lambda-1}\int_0^{r}P_{n_0 l_0}(x)P_{nl}(x)x^{\lambda}dx+r^{\lambda}\int_r^{\infty}P_{n_0 l_0}(x)P_{nl}(x)x^{-\lambda-1}dx\right] . \tag{22}$$

Upon averaging over the initial m_0 sublevels and integrating over the directions of the scattered electron and ejected electron, we have DW cross sections (neglecting exchange) as

$$\left[\frac{d\sigma}{d\varepsilon}\right]_{\mathrm{DW}}=k_1 k_2[(2l_0+1)k_0]^{-1}\sum_{m_0}\int|f(\mathbf{k}_1,\mathbf{k}_2)|^2 d\hat{\mathbf{k}}_1 d\hat{\mathbf{k}}_2$$
$$=16\pi k_1 k_2[(2l_0+1)k_0]^{-1}\sum_{l,m,l_1,l_2,m_2}(2l_1+1)\sum_{\lambda}[c^{\lambda}(l_1 0,l_2 m_2)c^{\lambda}(lm,l_0\, m_0=m-m_2)R^{\lambda}(k_0 l_1,n_0 l_0,k_1 l_2,nl)]^2 . \tag{23}$$

The exchange amplitude can be obtained from Eq. (6) by a similar substitution for the incident and scattered waves. However, such an analog of the Born-Oppenheimer exchange amplitude leads to unreasonably large cross sections. Therefore, we shall again resort to Ochkur's results [18], and assume that f and g are related by Eq. (7). However, since Eq. (7) was based on the plane-wave approximation, the use of this equation to determine g from f in a DW-type calculation must be viewed as a further step of approximation. Nevertheless the contribution to the ionization cross sections from g is usually much smaller than from f. Thus a DW calculation along with an Ochkur-like exchange should be a significant improvement over the Born-Oppenheimer ap-

proximation for ionization calculations. Following Eq. (7), we write

$$g/f=|\mathbf{k}_0-\mathbf{k}_1|^2/(k_0^2-k_2^2)$$
$$=(k_0^2+k_1^2-2k_0k_1\cos\theta_1)/(k_0^2-k_2^2)$$
$$=(a-b\cos\theta_1)\ , \tag{24}$$

where a and b are $(k_0^2+k_1^2)/(k_0^2-k_2^2)$ and $2k_0k_1/(k_0^2-k_2^2)$, respectively, and θ_1 is the angle $\hat{\mathbf{k}}_1$ makes with the z axis ($\hat{\mathbf{k}}_0$ being in the z direction).

Corresponding to the plane-wave Born-Ochkur cross section $(d\sigma/d\varepsilon)^+_{\rm BO}$, we express the cross sections based on the exchange-distorted-wave method with the Ochkur approximation (EDWO) as

$$\left[\frac{d\sigma}{d\varepsilon}\right]^+_{\rm EDWO}=k_1k_2[(2l_0+1)k_0]^{-1}$$
$$\times\sum_{m_0}\int|f+f(a-b\cos\theta_1)|^2d\hat{\mathbf{k}}_1d\hat{\mathbf{k}}_2$$
$$=I_0+I_1+I_2\ , \tag{25}$$

where I_0 is $[(a+1)^2+b^2/3]$ times the $(d\sigma/d\varepsilon)_{\rm DW}$ of Eq. (23), and

$$I_j=\alpha_j\sum_{l,m,\lambda,l_1,l_2,m_2,l_1',l_2'} i^{(l_1-l_2-l_1'+l_2')}c^\lambda(l_10,l_2m_2)c^\lambda(lm,l_0\,m_0=m-m_2)R^\lambda(k_0l_1,n_0l_0,k_1l_2,nl)$$
$$\times c^\lambda(l_1'0,l_2'm_2)c^\lambda(lm,l_0\,m_0=m-m_2)R^\lambda(k_0l_1',n_0l_0,k_1l_2',nl)c^j(l_2m_2,l_2'm_2),\quad j=1,2\ , \tag{26}$$

with

$$\alpha_1=-2b(a+1)\ , \tag{27}$$
$$\alpha_2=2b^2/3\ . \tag{28}$$

Equations (25) and (26) represent an exact transcription of Ochkur's formula to the DW calculation of ionization. However, a much simpler expression is obtained in Eq. (24) if we make use of the fact that for excitation to an optically allowed state as well as ionization, the scattering is strongly peaked in the forward direction. Thus we replace $|\mathbf{k}_0-\mathbf{k}_1|^2$ by $(k_0-k_1)^2$ in Eq. (24), so that

$$g=f\gamma\ , \tag{29}$$
$$\gamma=(k_0-k_1)^2/(k_0^2-k_2^2)\ , \tag{30}$$

and

$$\left[\frac{d\sigma}{d\varepsilon}\right]^+_{\rm EDWO}=k_1k_2[(2l_0+1)k_0]^{-1}(1+\gamma)^2$$
$$\times\sum_{m_0}\int|f(\mathbf{k}_1,\mathbf{k}_2)|^2d\hat{\mathbf{k}}_1d\hat{\mathbf{k}}_2\ . \tag{31}$$

We have made some test calculations using as an example the bound-state excitations from $O(3p^4\,^3P)$ to $O[2p^3(^4S)3s\,^3S]$ and to $O[2p^3(^4S)3d\,^3D]$. The use of Eq. (31) gives cross sections that are larger than the ones from Eqs. (25) and (26) by about 10% near the threshold. Beyond the threshold, the difference quickly decreases to the 3–5 % range with increasing incident energy. In view of such small differences, we use this simplified version of Ochkur's approximation in our calculations.

C. Ionization of oxygen atoms

In this paper we consider the ionization processes:

$$e^-+O(2p^4\,^3P)\rightarrow e^-+e^-+O^+(2p^3\,^4S,^2D,^2P)\ , \tag{32}$$

$$e^-+O[(2p^3\,^4S)n_0l_0\,^3L_0]\rightarrow e^-+e^-+O^+(2p^3\,^4S)\ . \tag{33}$$

We first determine the relevant orbitals of the oxygen atom (in the absence of the colliding electron) corresponding to the $O(2p^4\,^3P)$ and $O[(2p^3\,^4S)n_0l_0\,^3L_0]$ bound states and the $[O^+(2p^3\,^4S,^2D,^2P)+e^-]$ continuum states by the Hartree-Fock method with a frozen-core approximation in which the $1s$, $2s$, and $2p$ orbitals are treated as fixed and identical to the corresponding orbitals for the $(2p^4)^3P$ state of the oxygen atom as given by Clementi and Roetti [19]. Detailed procedures for calculating the n_0l_0 orbitals and the continuum-state orbitals have been described previously [27,28]. Analogous to the notation in Sec. II A, we use $\phi_0(\mathbf{r})$ for the active electron ($2p$ or n_0l_0) of the initial target state, and $\phi_f(\mathbf{k}_2,\mathbf{r})$ for the ejected electron. The latter is a superposition of angular momentum states of different l,m values and behave at large distance like a particle of momentum $\hbar\mathbf{k}$ as indicated in Ref. [28]. It is worth noting that the orthogonality condition is incorporated into the differential equation for the continuum-state orbitals [28], thereby obviating the arbitrary orthogonalization procedure at a later stage of the calculation.

Ionization is produced by the interaction of the colliding electron with the O atom

$$H_{\rm int}=-\frac{Z}{r_1}+\sum_{j=2}^{9}|\mathbf{r}_1-\mathbf{r}_j|^{-1}\ , \tag{34}$$

where the nuclear charge Z is 8, and we labeled the colliding electron as 1. Since $H_{\rm int}$ is independent of spin, we construct the spin eigenfunctions of the colliding system. For example, in the case of Eq. (32) we have for the initial state

$$\Psi_0(S,M|\mathbf{x}_1,\mathbf{x}_2,\ldots,\mathbf{x}_9)$$
$$=\mathcal{A}\sum_{\mu} C(\tfrac{1}{2},\mu,1,M-\mu;SM)$$
$$\times\phi_c(\tfrac{1}{2},\mu|\mathbf{x}_1)\Phi_0(1,M-\mu|\mathbf{x}_2,\ldots,\mathbf{x}_9)\ , \quad (35)$$

where $C(j_1,m_1,j_2,m_2;jm)$ is the Clebsch-Gordan coefficient, Φ_0 denotes the wave functions of the oxygen atom in the $(2p^4)^3P$ state, and the colliding electron is represented by ϕ_c, which will be described later. We use $\mathbf{x}_i$ to represent the spatial-spin coordinates, and $\mathcal{A}$ for the antisymmetrization operator. To construct the final-state wave function for Eq. (32), we first couple the O^+ ion function (Φ^+) with the spin-orbital of the ejected electron (ϕ_{ej}) to form the intermediate states Φ_{in}, i.e.,

$$\Phi_{in}(S_1M_1|\mathbf{x}_2,\ldots,\mathbf{x}_9)$$
$$=\mathcal{A}\sum_{\mu} C(\tfrac{1}{2},\mu,\tfrac{3}{2},M_1-\mu;S_1M_1)\phi_{ej}(\tfrac{1}{2},\mu,\mathbf{k}_2|\mathbf{x}_2)$$
$$\times\Phi^+(\tfrac{3}{2},M_1-\mu|\mathbf{x}_3,\ldots,\mathbf{x}_9)\ , \quad (36)$$

which are then coupled with the colliding electron function ϕ_c to form $\Psi_f(S'M'|\mathbf{x}_1,\ldots,\mathbf{x}_9)$. The scattering amplitudes are obtained by

$$\mathcal{T}^S=(1/2\pi)\int\Psi_f^*(SM|\mathbf{x}_1,\ldots,\mathbf{x}_9)H_{int}$$
$$\times\Psi_0(SM|\mathbf{x}_1,\ldots,\mathbf{x}_9)d\mathbf{x}_1\cdots d\mathbf{x}_9\ , \quad (37)$$

which are diagonal in (SM) and independent of M. As a consequence of Ψ_0 and Ψ_f being antisymmetrized, $\mathcal{T}^S$ includes both the direct f and exchange g amplitudes.

Next we sum the cross sections over S and M, and divide by $2(2S_1+1)$, the number of the possible initial spin states, S_1 being the spin of the initial atomic state, so that the results correspond to ionization by a beam of unpolarized electrons. By a straightforward calculation, we find

$$\frac{d\sigma}{d\varepsilon}=(k_1k_2/k_0)\sum_S[(2S+1)/2(2S_1+1)]$$
$$\times\int|\mathcal{T}^S|^2d\hat{\mathbf{k}}_1d\hat{\mathbf{k}}_2 \quad (38)$$
$$=(k_1k_2/k_0)\int(|f|^2-fg+|g|^2)d\hat{\mathbf{k}}_1d\hat{\mathbf{k}}_2\ , \quad (39)$$
$$f=-2K^{-2}C_{FP}\int\phi_0(\mathbf{r})e^{i\mathbf{K}\cdot\mathbf{r}}\phi_f^*(\mathbf{k}_2,\mathbf{r})d\mathbf{r}\ , \quad (40)$$

where C_{FP} stands for the coefficients of fractional parentage that arise due to the equivalent $2p$ orbitals in process (32), and is numerically equal to $\sqrt{\frac{4}{3}}$, $\sqrt{\frac{5}{3}}$, and 1, respectively, for the ^4S, ^2D, and ^2P final states of O^+ [29]. For process (33) the issue of fractional parentage does not arise, i.e., $C_{FP}=1$. The g amplitude is related to f through Eq. (7) or Eq. (29). Notice that there are no superscripts on the left-hand side of Eq. (38), since the cross section corresponds to ionization by unpolarized electrons.

To calculate the BO cross sections, $\phi_c(\mathbf{r})$ is taken as the incident plane wave $\exp(i\mathbf{k}_0\cdot\mathbf{r})$ in Ψ_0 and as $\exp(i\mathbf{k}_1\cdot\mathbf{r})$ in Ψ_f, and Eq. (7) is used to express g in terms of f. This gives

$$\left[\frac{d\sigma}{d\varepsilon}\right]_{BO}=(8\pi/k_0^2)C_{FP}^2\int_{K_{min}}^{K_{max}}(k_0^2-k_2^2)^{-2}[(k_0^2-k_2^2)^2-K^2(k_0^2-k_2^2)+K^4]|\langle n_0l_0|K|\varepsilon\rangle|^2K^{-3}dK\ . \quad (41)$$

For the EDWO calculations, ϕ_c takes on the more complicated form as given by Eqs. (17) and (18). In these equations the distorted partial waves are the solution of

$$\left[\frac{d^2}{dr^2}-\frac{l(l+1)}{r^2}-V(r)+k^2\right]\mathcal{P}_{kl}(r)=\sum_{n',l'}W_{n'l',kl}(r)P_{n'l'}(r)+\sum_{n''}c_{n''l}P_{n''l}(r)\ , \quad (42)$$

where the direct potential $V(r)$ is due to all eight atomic electrons in the oxygen atom for the appropriate initial state in process (32) or (33). Similarly, $W_{n'l',kl}P_{n'l'}$ represents the exchange interaction with all the target electrons. The last term in Eq. (42) is to ensure that $\mathcal{P}$ is orthogonal to all the bound nl orbitals via the Lagrange multiplier $c_{n''l}$. The details are further described in Ref. [28]. The distorted-wave functions of the projectile electron have the asymptotic form (as $r\to\infty$) of

$$\mathcal{P}_{kl}(r)\sim k^{-1}\sin(kr-\tfrac{1}{2}l\pi+\zeta_l)\ , \quad (43)$$

where ζ_l is the phase shift due to the potentials. As explained earlier, for the distorted-wave calculation we use the simplified version of the Ochkur exchange as given in Eq. (29). The EDWO cross sections then become

$$\left[\frac{d\sigma}{d\varepsilon}\right]_{EDWO}=16\pi k_1k_2C_{FP}^2[k_0(2l_0+1)]^{-1}\sum_{l,m,l_1,l_2,m_2}(2l_1+1)[1-\gamma+\gamma^2]\sum_{\lambda}[c^{\lambda}(l_1,0,l_2m_2)c^{\lambda}(lm,l_0\,m_0=m-m_2)$$
$$\times R^{\lambda}(k_0l_1,n_0l_0,k_1l_2,nl)]^2\ , \quad (44)$$

where γ is defined in Eq. (30). The total cross sections σ_{BO} and σ_{EDWO} are then obtained by integrating over ε as indicated in Eq. (15).

III. RESULTS

In order to check the numerical procedures we have computed the ionization cross sections of H($2s$) using the numerically tabulated functions for both the bound $2s$ state and the continuum (Coulomb) functions. In this test calculation we included the angular momenta of the ejected electron $l=0$ to 8. We were able to reproduce the cross sections computed by Prasad [30] within 4% for incident-electron energy from threshold to 200 eV.

In general a greater number of angular momenta l of the ejected electron are needed to achieve convergence as the incident-electron energy is increased. Also, the higher the quantum state from which ionization takes place, the more l's are needed. In this paper we used $l=0$ to 30 in the BO calculations for ionization of the oxygen atoms in the ground state and excited states ($n_0 l_0$) up to $n_0=6$, and used $l=0$ to 10 for the EDWO calculations that cover the ground state and excited states with $n_0=3$.

The integration with respect to K in Eq. (41) is carried out numerically. The smallest step size ΔK is 4×10^{-4}, and the step size is doubled after 10 quadrature points, except for the eleventh (last) region in which there are 30 points, for a total of 130 points. The rather small ΔK in the beginning is to take care of the steeply rising differential cross sections in the forward direction (i.e., toward small K) of the dipole-allowed transitions, to which all ionization processes belong. Similarly, with regard to ε integration in Eq. (15), we used the initial $\Delta\varepsilon=7.8125\times10^{-4}$ a.u., and doubled it after each region. There are eight regions with 10, 10, 10, 10, 40, 20, 20, and 80 quadrature points each.

A. Ionization of O($2p^4\,^3P$) to form $O^+(2p^3\,^4S,^2D,^2P)$

We have computed the Born (B) and BO cross sections, in the range of 17.5–500 eV of the incident-electron energy, of ionizing the ground state O($2p^4\,^3P$) atoms and leaving the $O^+(2p^3)$ ions in the three states ^4S, ^2D, and ^2P. The sum of these three cross sections, which corresponds to ionization of the ground-state oxygen atoms to form $O^+(2p^3)$ ions, is shown in Table I. We have also applied the EDWO method as well as the method of distorted waves without exchange (DW) to calculate the cross sections at incident energies 17.5–200 eV and the results are included in Table I. Comparison of the B with BO cross sections and of the DW with EDWO cross sections shows that the effect of electron exchange is to reduce the cross sections. At 25 eV this reduction amounts to 11% for B and 18% for DW, whereas at 200 eV, the BO is only 5% below the B cross section, and the difference between EDWO and DW is even smaller. Comparison of the BO and EDWO columns in Table I underscores the importance of the distortion of the projectile at low energies. The EDWO cross sections are smaller than the BO cross sections at 25 and 50 eV, but the order is reversed at 75–200 eV. Furthermore the EDWO and BO cross sections tend to merge at increasing energies.

TABLE I. Electron-impact ionization cross sections (in 10^{-16} cm^2) of ground-state oxygen atoms resulting in O^+ ions in the $(2p^3)^4S$, ^2D, and ^2P states calculated in the present work by using the method of exchange distorted waves with Ochkur's approximation (EDWO), by the method of distorted waves with no exchange (DW), by the Born-Ochkur (BO) approximations, and by the Born (B) approximation with no exchange.

	Cross section			
E (eV)	EDWO	DW	BO	B
25	0.171	0.210	0.326	0.367
50	0.952	1.027	0.996	1.123
75	1.287	1.347	1.252	1.367
100	1.360	1.405	1.293	1.411
125	1.337	1.369	1.272	1.274
150	1.276	1.302	1.223	1.310
200	1.134	1.149	1.091	1.152

The ionization cross sections of the O(^3P) atom have been calculated by several investigators. Peach [11,12] computed ionization cross sections resulting in $O^+(^4S,^2D,^2P)$ from the ground state. In the work of Peach [11] the function of Ref. [17] was used for the $2p$ orbital, and undistorted Coulomb functions of unit nuclear charge (hydrogenic Coulomb functions) were used for the ejected electron. The Born and Born-Ochkur methods were used; thus Peach's work is similar to the present one except for the use of the hydrogenic Coulomb functions. Later the author [12] discovered an error. As a result the cross sections [11] are to be reduced by a factor of 2. McGuire [13] computed the Born cross sections by using the wave functions based on the Herman-Skillman potential. Omidvar, Kyle, and Sullivan [14] used the scaled hydrogenic functions to compute the Born cross sections. Kazaks, Ganas, and Green [15] used the potential of the independent-particle model [31] to determine the wave functions from which the Born cross sections were obtained. Burnett and Rountree [16] reported a Born-approximation calculation using a set of very refined target wave functions. The latter four works [13–16] do not include the effect of electron exchange. In Table II we compare our results with those of the previous works. The columns labeled as BR (Burnett and Rountree [16]), OKS (Omidvar, Kyle, and Sullivan [14]), and KGG (Kazaks, Ganas, and Green [15]) are our best reading of the figures in the respective papers. The column Peach (Ref. [11]) shows the interpolation of Table 4 of Ref. [11] divided by 2 as corrected by Ref. [12]. Likewise, the column McGuire (Ref. [13]) is an interpolation of Table IV of Ref. [13]. The target wave functions used by Burnett and Rountree are more refined than ours. For the initial target state, they used a six-term CI wave function as opposed to our one-configuration Hartree-Fock work. To find the continuum functions for the ejected electron, Burnett and Rountree solved the close-coupling equations including the ^4S, ^2D, ^2P term manifold of the $O^+(2p^3)$ configuration whereas in our case the O^+ ion is taken to be in the $(2p^3)^4S$ state. Comparing the cross sections of Burnett and Rountree (BR), which were calculated by means of the Born approximation, listed in Table II with our cross sections calculated by the same method given in the last column of Table I,

TABLE II. Electron-impact ionization cross sections (in 10^{-16} cm^2) of oxygen atoms to form O^+ ions in the $(2p^3)^4S$, ^2D, and ^2P states calculated by the method of exchange distorted waves with Ochkur's approximation (EDWO) and by the Born-Ochkur approximation (BO) in this work at different electron energies E (in eV). Included for comparison are the cross sections from the earlier works by Burnett and Rountree (BR) [16], by Peach [11,12], by McGuire [13], by Omidvar, Kyle, and Sullivan (OKS) [14], and by Kazaks, Ganas, and Green (KGG) [15], as explained in the text. The last five sets of cross sections except those of Peach were calculated by means of the Born approximation (B) rather than the Born-Ochkur approximation (BO).

	This work						
E (eV)	EDWO	BO	BR (B)	Peach (BO)	McGuire (B)	OKS (B)	KGG (B)
25	0.171	0.326	0.38	0.192	0.55	0.55	
50	0.952	0.996	1.12	0.625	1.15	1.42	2.2
75	1.287	1.367	1.36	0.867	1.35	1.77	2.2
100	1.360	1.293	1.38	0.949	1.48	1.85	2.1
125	1.337	1.272	1.30	0.989	1.48	1.76	1.9
150	1.276	1.223	1.26	0.991	1.44	1.65	1.8
200	1.134	1.091	1.14	0.927	1.26	1.51	1.5
300		0.860		0.790	0.97	1.20	1.2

we see an agreement within 4%. This supports the accuracy of our wave functions. The cross sections listed under Peach (BO) in Table II, which were determined by Peach using the BO method, are substantially smaller than our BO results (about 30%). We believe that this is largely due to the different continuum wave functions (for the final target states) used to obtain the two sets of cross sections since the initial target-state wave functions are very similar in Peach's and our calculations. In the cases of the McGuire, OKS, and KGG calculations (Table II), the wave functions for both the initial and final target states are different from the ones used in the present work and their cross sections differ from our Born cross sections to varying extents.

Measurements of the ionization cross sections of the O atom were reported by Fite and Brackmann (FB) [4]. In a cross-beam experiment, they determined the ratio of the cross sections for ionizing atomic oxygen and molecular oxygen, $\sigma(O^+)/\sigma(O_2^+)$. Then utilizing the molecular ionization data of Tate and Smith [8], they obtained $\sigma(O^+)$. In a similar experiment Rothe *et al.* [5] measured ionization cross sections, and their results are in good agreement with those of FB [4]. In the experiment of Brook, Harrison, and Smith (BHS) [6], the charge-exchange process was used as the source of atomic beam so that the absolute cross sections were determined directly. Zipf [7], using the new data of O_2^+ ionization of Mark [9], revised the cross sections of FB. The "revised" cross sections are smaller than the uncorrected ones by a substantial margin below 100 eV, but above 100 eV the difference is only about 10%. Zipf [7] also determined the cross sections $\sigma(O^+)$ by normalizing his measurements to the data of BHS and the revised data of FB in the 100–300-eV range. The shape of the ionization function (a plot of cross sections versus incident energy) of Zipf [7] agrees quite well with BHS and also with FB above 100 eV.

In Fig. 1 we show the BO and EDWO cross sections of this work along with the experimental data of BHS and of FB as revised by Zipf [7]. The data of Zipf are not included because they are quite close to BHS. A cursory comparison indicates good agreement between the present calculation and experiments especially at energies above 70 eV. In the 70–150-eV range the difference is only about 3%, and at 200 eV the present calculation is about 10% smaller than the experimental value. A greater difference is found at lower energies; for example, at 50 eV our value is about 20% smaller than the experimental value. Below 70 eV there exists a substantial difference between the two sets of experimental data shown in Fig. 1. Since the BHS data came from a more recent experiment, we use them as the primary source of experimental data for comparison with our calculations.

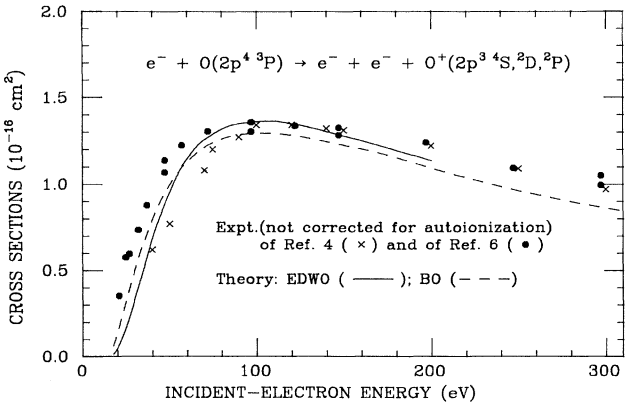

FIG. 1. Cross sections for electron-impact ionization of $O(2p^4\,^3P)$ to form $O^+(2p^3\,^4S,^2D,^2P)$ computed by the exchange-distorted-wave method with Ochkur's approximation (solid curve), and by the Born-Ochkur approximation (dashed curve). The experimental data from the work of Brook, Harrison, and Smith [6] are designated by dots (●), and those from the work of Fite and Brackmann [4] as revised by Zipf [7] are designated by crosses (×). The experimental cross sections shown in the graph have not been corrected for the autoionization contributions (see Fig. 2).

For a more definitive assessment of the comparison of our calculation with experiments, two points must be considered. The first is that the experimental cross sections include the effects of autoionization as well as the direct ionization, whereas only the latter is considered in the theory. While Brook, Harrison, and Smith [6] indicated that their experimental data show no discernible evidence of autoionization, detailed examinations of the ionization yield and optical emission of the autoionizing states [32–34] show that the influence of autoionization on the measured cross sections must be taken into consideration. In particular autoionization via the $O[2s^2 2p^3(^2P)3s''\,^3P^\circ]$ and $O[2s2p^5\,^3P^\circ]$ states are found to contribute significantly to the observed ionization cross sections. Since the $^3P^\circ$ symmetry cannot be realized from the $O^+[2p^3\,^4S]$ ion plus an additional (unbound) electron, the autoionization rates of the above-mentioned $^3P^\circ$ states are much reduced and become comparable to the radiative emission rates. Dehmer, Luken, and Chupka [32] experimentally determined the ratio of the autoionization rate to the emission rate to be nearly equal to unity for both the $3s''\,^3P^\circ$ and $2s2p^5\,^3P^\circ$ states, i.e., half of the population in these states decay by autoionization and the other half by emission. Zipf and Kao [33], from their experimental emission cross sections and the branching ratios of Dehmer, Luken, and Chupka [32], conclude that autoionization contributes substantially to the production of $O^+(^4S)$ ions by electron impact. In a more recent electron-impact energy-loss experiment, Vaughan and Doering [34] determined the excitation cross sections for several states of atomic oxygen including the two autoionizing $^3P^\circ$ states mentioned earlier and the $2p^3(^2D)4d'\,^3P^\circ$ state at incident-electron energies between 30 and 200 eV. The excitation functions for these states are seen to peak at 50 eV [34]. Applying the branching ratios of Dehmer, Luken, and Chupka, referred to earlier, to the excitation cross sections of Vaughan and Doering for the $3s''\,^3P^\circ$ and $2s2p^5\,^3P^\circ$ states, we can determine the contribution to the ionization cross sections due to autoionization through the $3s''\,^3P^\circ$ and $2s2p^5\,^3P^\circ$ states. The excitation cross section for the $2p^3(^2D)4d'\,^3P^\circ$ state is much smaller than those of the other two $^3P^\circ$ states mentioned above; thus even if we assume that the $2p^3(^2D)4d'\,^3P^\circ$ state decays by autoionization entirely, this autoionization channel makes a much smaller contribution to the measured ionization cross section compared to the $3s''\,^3P^\circ$ and $2s2p^5\,^3P^\circ$ channels. Indeed Dehmer, Luken, and Chupka [32] indicated that the $2s^2 2p^3(^2D)3d'\,^3P^\circ$ state decays primarily by autoionization. Thus we assume a 100% autoionization decay for the $2s^2 2p^3(^2D)4d'\,^3P^\circ$ state in order to determine the contribution from this channel to the ionization cross section. From this analysis we obtain the autoionization contributions to the observed ionization cross sections as 0.068, 0.151, 0.090, 0.071, and 0.048×10^{-16} cm^2 at 30, 50, 100, 150, and 200 eV, respectively. This correction is applied to the measured ionization cross sections of BHS in order to remove the autoionization contribution. The second point is that even in the absence of autoionization, the experimental data include also the results of inner-shell ionization. The ionization energy for the $2s$ electrons in the oxygen atom is about twice as large as the ionization energy for the $2p$ electrons. Thus we expect the ionization cross sections for the $2s$ electrons to be small, but not negligible, in comparison to those of the $2p$ electrons. Accordingly we have calculated the Born-Ochkur cross sections for the inner-shell ionization process:

$$e^- + O(2s^2 2p^4\,^3P) \rightarrow e^- + e^- + O^+(2s2p^4\,^4P, ^2P)\,. \quad (45)$$

Here the wave functions for the ionization electron are the Hartree-Fock continuum-state functions of an electron in the presence of the $O^+(2s2p^4\,^4P)$ or $O^+(2s2p^4\,^2P)$ ion. The resulting cross sections, in units of 10^{-16} cm^2, are 0.059 at 50 eV, 0.136 at 100 eV, 0.145 at 150 eV, and 0.138 at 200 eV, amounting to about 10% of the cross sections for ionizing the $2p$ electron, i.e., process (32). Calculations of cross sections for process (45) have been published by Peach in 1970 [11]. The cross sections given there are much larger than ours. To describe the ionized electron, Peach adopted the hydrogenic Coulomb functions as opposed to the Hartree-Fock continuum-state functions in our work. The use of the hydrogenic Coulomb functions to calculate ionization cross sections for the oxygen atom neglects the influence of the extended charge distribution of the passive electrons on the ionized electron, and therefore may not yield accurate cross sections for ionizing the inner-shell $2s$ electrons especially in view of the penetrating character of the s orbitals. To examine this issue we have recalculated the cross sections for process (45) replacing the Hartree-Fock continuum-state wave functions for the ionized electron by the hydrogenic Coulomb functions. This yields cross sections of 0.166, (50 eV), 0.412, (100 eV), 0.446 (150 eV), and 0.358 (200 eV) in units of 10^{-16} cm^2, which are about three times as large as the cross sections calculated by using the Hartree-Fock continuum functions, but are much closer to Peach's data. Direct comparison of these values with Peach's results is complicated by the fact that the cross sections presented in Peach's paper include the ionization of the $2s$ electrons as well as the extrapolated autoionization cross sections. The cross sections from Peach's work which we obtained by interpolating the energy scale are, for instance, 0.59×10^{-16}, 0.60×10^{-16}, and 0.57×10^{-16} cm^2 at 100, 150, and 200 eV, respectively. These values are understandably larger than, but nevertheless reasonably close to, our $2s$ ionization cross sections calculated by using the hydrogenic Coulomb functions. It is not necessary for us to calculate the autoionization cross sections since we have already removed the autoionization contributions to the experimental data as described earlier in this paragraph.

In Fig. 2 we present the experimental ionization cross-section data [6] that have been corrected for autoionization. For comparison with these "corrected" experimental data, our theoretical ionization cross sections shown here include the ionization of the $2s$ electrons in addition to the ionization of the $2p$ electrons. The theoretical values are seen to be about 15% larger than the experimental values for incident-electron energies between 70 and 200 eV, but become smaller than the experimental

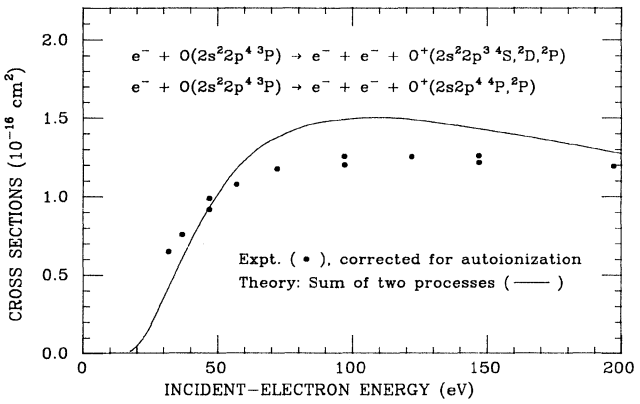

FIG. 2. Sum of the cross sections for electron-impact ionization of $O(2s^2 2p^4\,{}^3P)$ to form $O^+(2s^2 2p^3\,{}^4S,{}^2D,{}^2P)$ computed by the exchange-distorted-wave method with Ochkur's approximation and for ionization of $O(2s^2 2p^4\,{}^3P)$ to form $O^+(2s2p^4\,{}^4P,{}^2P)$ computed by the Born-Ochkur method (solid curve) as compared to the experimental data (●), which are taken from the work of Brook, Harrison, and Smith [6], corrected for autoionization contribution by using the measurements of Vaughan and Doering [34], as described in the text.

values below 50 eV. We find the overall agreement between theory and experiment reasonably good and satisfactory.

B. Ionization of $O[2s^2 2p^3(^4S)n_0 l_0\,{}^3L_0]$ to form $O^+(^4S)$

We have calculated the cross sections for ionizing the excited oxygen atoms $O[2p^3(^4S)n_0 l_0\,{}^3L_0]$ by electron impact. In Figs. 3 and 4, we show the BO and EDWO cross sections for $n_0 l_0 = 3s$, $3p$, and $3d$. In each case the peak of the ionization function occurs immediately above the threshold (8.0 eV for $3s$, 6.0 eV for $3p$, and 4.0 eV for $3d$),

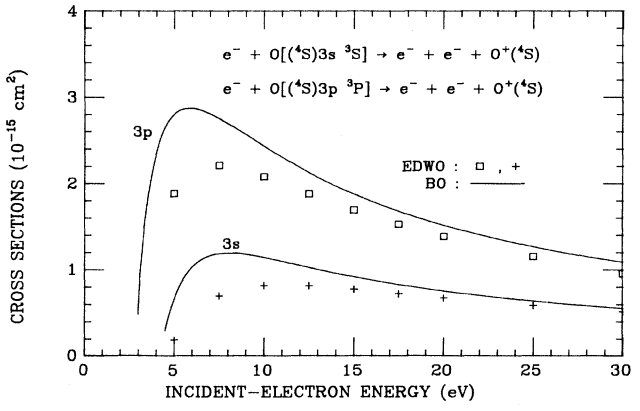

FIG. 3. Cross sections for electron-impact ionization of $O[2p^3(^4S)3s\,{}^3S]$ and $O[2p^3(^4S)3p\,{}^3P]$ to form $O^+(^4S)$ computed by the Born-Ochkur approximation (solid curves). Those computed by the exchange-distorted-wave method with Ochkur's approximation are shown by crosses (+) for ionizing orbital $n_0 l_0 = 3s$, and by squares (□) for $n_0 l_0 = 3p$.

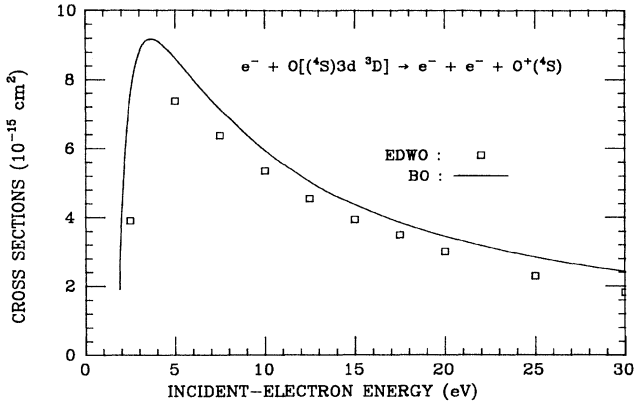

FIG. 4. Cross sections for electron-impact ionization of $O[2p^3(^4S)3d\,{}^3D]$ to form $O^+(^4S)$ computed by the Born-Ochkur approximation (solid curve) and by the exchange-distorted-wave method with Ochkur's approximation (□).

in marked contrast to ionization of the ground state where the peak cross section occurs at about 100 eV. Such a characteristic distinction between ionization from the ground state and from excited states is also seen for the H and He atoms. The ionization functions for $H(2s)$ and $H(2p)$ peak around 8–13 eV [30], whereas the maximum of the $H(1s)$ ionization function occurs between 80 and 100 eV. Similarly the ionization functions for $He(2^1S)$ and $He(2^3S)$ peak around 10 eV [35], as opposed to the peak position in the 80–100-eV range for $He(1s)$ [36]. As in the case of ionization from the ground state, the EDWO cross sections are substantially smaller than the BO cross sections at low energies. However, the two sets of cross sections become much closer to each other with increasing energy as can be seen in Table III.

TABLE III. Comparison of the BO and EDWO cross sections for ionization of oxygen atoms in the $[2p^3(^4S)n_0 l_0]^3L_0$ states. For each incident-electron energy E, there are two entries: the first is the BO and the second the EDWO cross sections (in 10^{-15} cm^2).

	Cross section		
E (eV)	$3s$	$3p$	$3d$
2.5			7.49
			3.90
5.0	0.659	2.80	8.62
	0.189	1.88	7.36
7.5	1.19	2.75	7.14
	0.700	2.21	6.37
10.0	1.14	2.43	5.93
	0.818	2.08	5.34
12.5	1.02	2.12	5.03
	0.815	1.88	4.54
15.0	0.917	1.88	4.36
	0.774	1.69	3.93
17.5	0.827	1.68	3.85
	0.724	1.53	3.49
20.0	0.752	1.51	3.44
	0.674	1.39	3.00

We have extended the BO calculation to $n_0 l_0$ up to (6,5). The general shape of the ionization function remains the same except for a small inward shift in the peak. We have fitted the ionization function for each $n_0 l_0$ from 7.5 to 500 eV to the relation

$$\sigma = c_1 E^{-1} \ln E + c_2 E^{-1} + c_3 E^{-2} , \quad (46)$$

where the incident-electron energy E is in eV and the cross section in cm^2. The numerical values of c_1, c_2, and c_3 are given in Table IV. As in the case of ionization of the ground-state oxygen atom, one may consider the contributions to the ionization cross sections of the $O[2s^2 2p^3(^4S)n_0 l_0]$ atoms from the inner-shell ionization, i.e., removal of the $2s$ or $2p$ electrons. Our Born-Ochkur calculations give a peak cross section of 1.0×10^{-16} cm^2 for removal of a $2p$ electron and 7×10^{-18} cm^2 removal of a $2s$ electron from the excited $O[2s^2 2p^3(^4S)3s\ ^3S]$ atom. They are much smaller than the cross sections for removing the outer electron from $O[2s^2 2p^3(^4S)n_0 l_0]$, e.g., 1.2×10^{-15} cm^2 for $n_0 l_0 = 3s$, 2.9×10^{-15} cm^2 for $n_0 l_0 = 3p$, and 9.2×10^{-15} cm^2 for $n_0 l_0 = 3d$. Thus the inner-shell ionization will not be taken into consideration in our study for ionization of the excited oxygen atoms.

Finally it should be recalled that in the present calculation the initial states are triplet states. Although we did not make a separate set of calculations for the case of quintet initial states, we expect the latter cross sections to be rather close to the former set. In the radiative-recombination calculation [28] involving the above two sets of triplet and quintet states, the difference in cross sections were found to be about 15% for $n_0 = 3$, 10% for $n_0 = 4$, and less still for higher n_0.

TABLE IV. Values of the coefficients in the Bethe-type expansion [Eq. (46)] of the ionization cross sections (in cm^2) for the oxygen atoms in the $[2p^3(^4S)n_0 l_0]^3L_0$ states as a function of the incident-electron energies (in eV). Number inside the brackets indicates the power of 10.

$n_0 l_0$	c_1	c_2	c_3
3,0	1.135[−15]	1.458[−14]	−5.797[−14]
4,0	2.682[−15]	4.172[−14]	−7.230[−14]
5,0	3.760[−15]	8.517[−14]	−8.563[−14]
6,0	1.473[−15]	1.480[−13]	−1.096[−13]
3,1	1.541[−15]	3.044[−14]	−9.684[−14]
4,1	7.842[−15]	5.170[−14]	−5.615[−14]
5,1	1.522[−14]	9.016[−14]	−5.832[−14]
6,1	1.709[−14]	1.458[−13]	−5.230[−14]
3,2	4.265[−15]	6.280[−14]	−1.380[−14]
4,2	1.354[−14]	8.649[−14]	−6.529[−14]
5,2	2.437[−14]	1.202[−13]	−3.767[−14]
6,2	1.627[−14]	2.028[−13]	−6.385[−14]
4,3	7.231[−15]	1.084[−13]	−9.185[−14]
5,3	1.688[−14]	1.444[−13]	−6.222[−14]
6,3	1.791[−14]	2.013[−13]	−5.938[−14]
5,4	7.499[−15]	1.696[−13]	−8.738[−14]
6,4	1.088[−14]	2.239[−13]	−7.515[−14]
6,5	7.535[−15]	2.309[−13]	−7.217[−14]

IV. SUMMARY AND CONCLUSIONS

We have calculated the electron-impact ionization cross sections of producing the O^+ ions (in the $2p^3$ configuration) from the ground state $O(^3P)$ atom by the BO and by EDWO approximations. For comparison similar calculations neglecting electron exchange have been performed (the B and DW approximations). The continuum wave functions of the ionized electron were computed by the Hartree-Fock method with full allowance for the Coulomb and exchange interactions with the remaining electrons and the nucleus of O^+.

The EDWO gives significantly smaller cross sections than does BO at low electron energies. For example, at 30 eV the EDWO cross section is smaller by 15%, and at lower energy smaller still by a greater percentage. However, between 70–200 eV, the difference is about 10% or less, and the two sets of cross sections tend to merge at high incident energy.

By accounting for the distortion of the projectile electron by the target and using the proper continuum functions, we made a significant improvement over the previous calculations, which are within the stage of the B or BO approximation and, in most cases, with the hydrogenic Coulomb functions, so that we can make a quantitative comparison with the experimental measurements [4–7]. In the energy range of 50–200 eV the present EDWO cross sections agree with the experimental measurements (with correction for autoionization contributions and inner-shell ionization) within about 15% or less. Below 50 eV the discrepancy becomes larger. One may speculate that the larger discrepancy at low energies may be partly due to a possible increase in the percentage uncertainty of the experimental measurements on account of the cross sections being much smaller and varying steeply with energy. It should also be pointed out that in our BO and EDWO calculations, the polarization of the target-state wave functions by the incident electron is neglected. This target polarization effect is more important at very low incident-electron energies, and may be partly responsible for the discrepancy between theory and experiment at very low energies. We may also add that at energies above 37 eV, ionization may take place through channels in which the O^+ ion is initially formed in an excited configuration such as $2p^2 3s$. However, contributions from these channels, which involve two active electrons and are not included in our calculations, to the ionization cross sections are unimportant when we are discussing accuracy on the level of 15%.

We have computed BO cross sections of ionizing Rydberg oxygen atoms in the $[2p^3(^4S)n_0 l_0]^3L_0$ for $(n_0 l_0) = (3,0)$ through $(n_0 l_0) = (6,5)$. These cross sections are sharply peaked within a few eV above the threshold in contrast to the ionization function of the ground state, which shows a broad peak around 100 eV. Similar characteristic distinction between ionization of the ground state and excited states has also been reported for the H and He atoms. For comparison we have used the EDWO approximation to calculate the ionization cross sections for the Rydberg oxygen atoms with $n_0 = 3$. The EDWO cross sections are significantly smaller than

their BO counterparts at low incident energies but above 15 eV or so the two sets become quite close to each other.

To summarize the large amount of the BO ionization cross-section data for the Rydberg oxygen atoms, we present the cross sections in the form of a Bethe-type expansion. Detailed information about ionization processes involving excited oxygen atoms is important in studies of radiation in the upper atmosphere and in modeling and diagnostics of plasmas.

ACKNOWLEDGMENT

The part of the work done at the University of Wisconsin was supported by the Phillips Laboratory (Air Force Systems Command).

[1] L. J. Kieffer and G. H. Dunn, Rev. Mod. Phys. **38**, 1 (1966).
[2] R. R. Laher and F. R. Gilmore, J. Phys. Chem. Ref. Data **19**, 277 (1990).
[3] K. L. Bell, H. B. Gilbody, J. G. Hughes, A. E. Kingston, and F. J. Smith, J. Phys. Chem. Ref. Data **12**, 891 (1983).
[4] W. L. Fite and R. T. Brackmann, Phys. Rev. **113**, 815 (1959).
[5] E. W. Rothe, L. L. Marino, R. H. Neynaber, and S. M. Trujillo, Phys. Rev. **125**, 582 (1962).
[6] E. Brook, M. F. A. Harrison, and A. C. H. Smith, J. Phys. B **11**, 3115 (1978).
[7] E. C. Zipf, Planet. Space Sci. **33**, 1303 (1985).
[8] J. T. Tate and P. T. Smith, Phys. Rev. **39**, 270 (1932).
[9] T. D. Mark, J. Chem. Phys. **63**, 3731 (1975).
[10] M. J. Seaton, Phys. Rev. **113**, 814 (1959).
[11] G. Peach, J. Phys. B **1**, 1088 (1968); **3**, 328 (1970).
[12] G. Peach, J. Phys. B **4**, 1670 (1971).
[13] E. J. McGuire, Phys. Rev. A **3**, 267 (1971).
[14] K. Omidvar, H. L. Kyle, and E. C. Sullivan, Phys. Rev. A **5**, 1174 (1972).
[15] P. A. Kazaks, P. S. Ganas, and A. E. S. Green, Phys. Rev. A **6**, 2169 (1972).
[16] T. Burnett and S. P. Rountree, Phys. Rev. A **20**, 1468 (1979).
[17] E. Clementi, *Tables of Atomic Wave Functions* (IBM, San Jose, CA, 1965).
[18] V. I. Ochkur, Zh. Eksp. Teor. Fiz. **47**, 1746 (1964) [Sov. Phys. JETP **20**, 1175 (1965)].
[19] E. Clementi and C. Roetti, At. Data Nucl. Data Tables **14**, 177 (1974).
[20] R. K. Peterkop, *Theory of Ionization of Atoms by Electron Impact* (Colorado Associated University Press, Boulder, CO, 1977).
[21] M. R. H. Rudge and M. J. Seaton, Proc. Phys. Soc. London **83**, 680 (1964); Proc. R. Soc. London, Ser. A **283**, 262 (1965).
[22] M. R. H. Rudge, Rev. Mod. Phys. **40**, 564 (1968).
[23] F. W. Byron Jr. and C. J. Joachain, Phys. Rep. **179**, 211 (1989); R. J. W. Henry, *ibid.* **68**, 1 (1981).
[24] S. M. Younger, Phys. Rev. A **22**, 111 (1980).
[25] D. H. Madison, R. V. Calhoun, and W. N. Shelton, Phys. Rev. A **16**, 552 (1977); Y. Itikawa and K. Sakimoto, *ibid.* **31**, 1319 (1985).
[26] E. U. Condon and G. H. Shortley, *The Theory of Atomic Spectra* (Cambridge University Press, Cambridge, England 1963), p. 175.
[27] S. Chung, C. C. Lin, and E. T. P. Lee, J. Quant. Spectrosc. Radiat. Transfer **36**, 19 (1986).
[28] S. Chung, C. C. Lin, and E. T. P. Lee, Phys. Rev. A **43**, 3433 (1991).
[29] B. W. Shore and D. H. Menzel, *Principles of Atomic Spectra* (Wiley, New York, 1968), pp. 378–91.
[30] S. S. Prasad, Proc. Phys. Soc. London **87**, 393 (1966).
[31] A. E. S. Green, D. L. Sellin, and A. S. Zachor, Phys. Rev. **184**, 1 (1969).
[32] P. M. Dehmer, W. L. Luken, and W. A. Chupka, J. Chem. Phys. **67**, 196 (1977).
[33] E. C. Zipf and W. W. Kao, Chem. Phys. Lett. **125**, 394 (1986).
[34] S. D. Vaughan and J. P. Doering, J. Geophys. Res. **93**, 289 (1988).
[35] D. Ton-That, S. T. Manson, and M. R. Flannery, J. Phys. B **10**, 621 (1977).
[36] K. L. Bell and A. E. Kingston, J. Phys. B **2**, 1125 (1969).